Effect of fluctuation in step size on actin-myosin sliding motion

Yuki Kagawa*
Department of Electrical Engineering & Bioscience, Waseda University, 3-4-1, Okubo, Shinjuku-ku, Tokyo, 169-8555, Japan
(Received 25 September 2006; published 24 January 2007)

It is possible that the step size, or power stroke, of a skeletal muscle myosin is not constant; rather, it fluctuates for each force generation. The estimated widths of the fluctuation are as large as the estimated values of the step size. Although such non-negligible fluctuation is presumed to affect the sliding motion, these effects remain unclear. We examined a system driven by a single myosin molecule sliding along an actin filament to reveal its basic effects. First, we calculated the sliding velocity of the system for each fluctuation width and found that the mean velocity increased with the fluctuation width. We also found that the estimated fluctuation widths satisfied the conditions for maximizing the sliding velocity. Next, we examined the sliding motion along a heterogeneous filament, on which binding sites for myosins were distributed randomly. We found that the loss in sliding velocity that was attributable to heterogeneity of the filament became small when fluctuation in the step size existed. This finding implied that the fluctuation stabilized velocity sliding along possible heterogeneous filaments. These benefits of fluctuation in step size might be used in biological systems, such as a muscle system, and are applicable to fabricated micromachines.

DOI: 10.1103/PhysRevE.75.011923 PACS number(s): 87.16.Nn, 87.19.Ff, 05.40.−a

I. INTRODUCTION

Muscle contraction is caused by cyclical interactions between myosin motor proteins and actin filaments. The myosin generates a piconewton-scale force and moves the filament along its axis direction for a unitary distance when a single myosin interacts with an actin filament. Simultaneously, the acto-myosin hydrolyzes an ATP and releases ADP and inorganic phosphate (Pi). Such a conceptual image for the interaction has been obtained directly through single-molecule experiments over the last few decades [1–8] (for reviews, see Refs. [9,10]). In this paper, the displacement of the filament produced by the interaction in these single-molecule experiments is called the step size.

In a previous study [11], we presented the possibility that the step size of a skeletal muscle myosin II is not constant. Rather, it fluctuates for each interaction. We presumed that the step size can vary according to the following several factors: (i) variation in the conformation of myosin when it begins a force generation [12], (ii) variation in the relative orientation between actin filament and myosin head [13], and (iii) variation in the number of possible smaller steps, which comprise a single step size [5]. Recent experiments using an intact muscle cell suggest that step size varies with environmental factors such as load [14] and temperature [15]. Therefore, local environmental changes around myosins might cause the fluctuation.

Estimated fluctuation widths of step sizes are shown in Table I (see the column of w). These values are as large as the values of estimated step size (the column of Δ_m). In this table, we also present data for Chara myosin, a class XI myosin found in green algae [16]. This myosin is double headed, but did not show successive steps in the single-molecule experiment [17], like a skeletal muscle myosin II. In the Appendix, we show how to estimate the fluctuation width. These estimated values are considerably large. Therefore, the fluctuation in step size is presumed to affect the sliding motion of actin-myosin systems. However, little is known about the effects of the fluctuation on the sliding motion.

In some biological systems, fluctuation, or noise, plays a beneficial role. For example, the sensitivity of sensory neurons is optimized by a stochastic resonance in neural systems [19,20]. As another example, the increased noise in the transcription of a regulatory protein increases the variability in the target gene expression among cells. That increased variability implies that noise has a role in cell differentiation [21]. Consequently, we expect that the fluctuation in step size also plays some beneficial role in actin-myosin sliding motion.

A system that is driven by a single myosin molecule sliding along an actin filament is considered to reveal the effects of the fluctuation in step size on the sliding motion. For simplicity, the myosin is assumed to be single headed. First, we construct two simple motional models, and introduce the fluctuation in step size to these models. Next, we numerically calculate and theoretically derive the sliding velocity as a function of the fluctuation width. We also calculate the velocity of sliding along a heterogeneous filament and examine the effect of the fluctuation on the sliding motion. Finally, we compare theoretical results with corresponding experimental data and discuss whether the fluctuation in step size plays some beneficial role in biological systems, particularly in muscle systems.

II. MODELS

We constructed two motional models to elucidate the effects of the fluctuation in step size on the actin-myosin sliding motion. The first model is so simple that we can derive the analytical expressions of mean sliding velocities with and without the fluctuation. We constructed another model to verify that the effects of the fluctuation on the sliding motion

*Electronic address: ykagawa@aoni.waseda.jp

TABLE I. Estimated values of model parameters using single molecule experimental data sets.

Sample no.	Myosin	L (nm)	Δ_m (nm)	Δ_m/L	w (nm)	$w_{\max}$ (nm)	Reference
1	Skeletal muscle	36	15[a]	0.42	12–17[b]	15	[13]
2	Skeletal muscle	36	5.4[a]	0.15	5–6[b]	5.4	[18]
3	Chara	36	18[a]	0.50	13[c]	18	[17]

[a]Given in the corresponding references.
[b]Estimated in a previous study [11].
[c]Estimation given in the Appendix.

are independent of model details. This model includes stochastic processes of attachment and detachment of myosin to and from the actin filament. Thus, the sliding motion is more natural than that in the first model. Following the construction of these two basic models, we expand the models by introducing the fluctuation in step size and a heterogeneous actin filament.

A. The first motional model

We construct the first motional model (model 1) as follows [see Figs. 1(a)–1(e)]. This model consists of a single-headed myosin, an actin filament, binding sites for myosins on the actin filament, and a cargo. We assume that the myosin can attach to the actin filament at only one binding site, and that the cargo and the myosin are rigidly connected. The binding sites are placed at uniform intervals of L. Myosin can assume one of two conformations (straight or bent) depending on the absence or presence of the ligand (ATP or ADP·Pi). Figure 1(a) shows the state immediately preceding the force generation. In that state, a myosin attaches to a binding site with an ADP·Pi. Immediately after the attachment, the myosin releases the ADP·Pi and changes its conformation to the bent one [Fig. 1(b)]. Consequently, the rigidly connected cargo moves forward for a horizontal distance of Δ. This distance corresponds to the step size. The myosin attaches to the actin rigorously until an ATP binds to the myosin. The affinity of the myosin for the actin is reduced and it detaches from the binding site [Figs. 1(b) to 1(c)] when an ATP binds to the myosin. The detachment rate is denoted as ν. After the detachment, the myosin reverts to the straight conformation [Figs. 1(c) to 1(d)]. The myosin-cargo system diffuses along the actin filament with a diffusion constant of D until it encounters one binding site. Whenever the system encounters one of the binding sites, it always attaches to the site and never passes one. Thus, the system can slide for a distance of 0 or L [Figs. 1(a) to 1(a) or Figs. 1(a) to 1(e), respectively] for each force generation. Repeating this chemomechanical cycle, the myosin-cargo system slides along the actin filament.

The cargo corresponds to the thick filament of muscle. In actual biological conditions, however, the thick filament contains many myosins and is not driven by a single myosin. Thus, the present model corresponds to a special case in which only one myosin can generate force and the other myosins are weakly bound to the filament. This weakly binding interaction between the myosins and the actin filament prevents the system from diffusing away, and affects the sliding motion of the system as friction, known as molecular friction [22,23]. The diffusion constant of the system D includes the effect of this molecular friction.

Using this simple model, we can (i) characterize the sliding motion with only four parameters L, Δ, ν, and D; (ii) easily introduce the fluctuation in the step size (see below); and (iii) derive an analytical expression for the mean sliding velocity with and without step size fluctuation.

B. Second motional model

The second motional model (model 2) is basically the same as model 1, except for the following assumptions: (i) the conformational change of a myosin is caused by the release of energy stored in the strain x of the myosin; and (ii) the myosin attaches to and detaches from binding sites in a stochastic fashion. The myosin is assumed to generate a force $-Kx$ when its strain is equal to x, and the strain immediately before the force generation is assumed to be $-\Delta$ [see Fig. 1(f)], where K is the stiffness of the myosin and Δ corresponds to the step size. Therefore, the dynamics of the strain is given by the Langevin equation

$$\gamma\frac{dx(t)}{dt} = -Kx(t) + (2D)^{1/2}\gamma\xi(t), \tag{1}$$

where γ and D respectively denote the coefficient of viscous drag and the diffusion constant of the myosin-cargo system.[1] Also, $\xi(t)$ is zero-mean white Gaussian noise $\langle\xi(t)\rangle=0$, $\langle\xi(t)\xi(t')\rangle=\delta(t-t')$. Here we consider the case of a heavily overdamped environment. Thus the inertial term is neglected. By calculating Eq. (1) with the initial condition of $x(0)=-\Delta$, the temporal change of the system position during force generation is given by that of the strain $x(t)$.

The myosin is assumed to detach from the binding site [Figs. 1(b) to 1(c)] when the strain is zero or positive ($x \geq 0$) with a rate constant of k_{off} [Fig. 1(g)]. After the detachment, the myosin changes back to the straight conformation and diffuses along the actin filament [Fig. 1(d)]. When the

[1]To satisfy Einstein's relation between γ and D, D in Eq. (1) should not include the effect of molecular friction caused by other myosins weakly bound to the actin filament. If we consider this effect, the molecular friction term must be added to Eq. (1). As a result, the effective diffusion constant of the system D_{eff} becomes smaller than D. Note that D in model 1 corresponds to D_{eff} here.

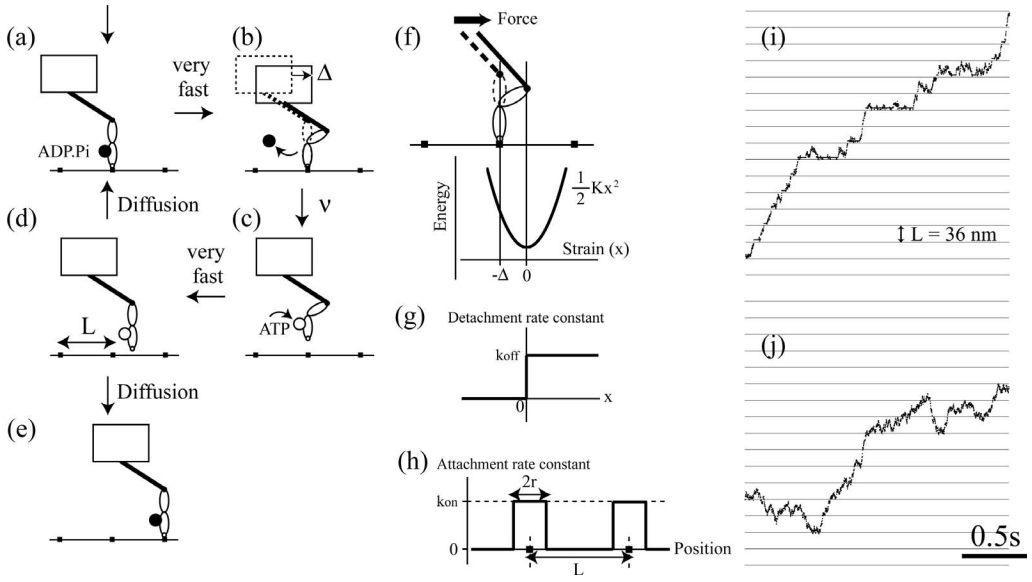

FIG. 1. Motional models. (a)–(e) Model 1. When a myosin head (two connected ovals) attaches to one of the binding sites on an actin filament (closed squares on a horizontal line) with ADP·Pi (closed circle), it releases the ADP·Pi and changes its conformation [(a) to (b)]. As a result, a cargo (a rectangle) moves forward (right) along the filament for a distance of Δ, corresponding to the step size. In this state, the myosin waits for an ATP to bind. When an ATP (open circle) binds to the myosin, it detaches from the binding site [(b) to (c)]. The detachment rate constant is assumed to be ν. After the detachment, the myosin structure reverts rapidly to its former conformation [(c) to (d)]. The myosin-cargo system diffuses along the actin filament (d) until it attaches to one of two binding sites, i.e., the initial and the forward ones [(a) and (e), respectively]. (f)–(h) Model 2. (f) When a myosin head changes its conformation [see (a) to (b)], the myosin generates a force of $-Kx$, where x and K, respectively, denote the strain and the stiffness of the myosin. After the force generation, the myosin has no strain, i.e., $x=0$. The parabola shows the energy stored in the myosin plotted against the strain x. The energy difference between preforce and postforce generation is determined by the step size Δ as $K\Delta^2/2$. (g) The strain-dependent rate constant (thick lines) for detachment of a myosin from a binding site [corresponding to (b) and (c)]. $k_{\text{off}}=1\ \text{ms}^{-1}$ is used. (h) The position-dependent rate constant (thick lines) for attachment of a strained myosin to binding sites [corresponding to (d) to (a) or (d) to (e)]. $L=36$ nm, $r=0.5$ nm, and $k_{\text{on}}=1\ \text{ms}^{-1}$ are used. (i) and (j) Example time series of the system under the conditions of $\Delta=5$ nm, $L=36$ nm, and $D=4\ \text{nm}^2\ \text{ms}^{-1}$ in models 1 and 2, respectively. For calculations, $\nu=0.1\ \text{ms}^{-1}$ is used in (i), and $\gamma=1\ \mu\text{g ms}^{-1}$, $k_{\text{off}}=1\ \text{ms}^{-1}$, $k_{\text{on}}=1\ \text{ms}^{-1}$, and $r=0.5$ nm are used in (j). Positions of the system (ordinate) were plotted against time (abscissa). The horizontal gridlines are drawn with spacing of 36 nm (=L). The bar in (j) corresponds to 0.5 s.

myosin diffuses to the domain of $[X_B-r, X_B+r]$, where X_B is the position of a binding site, the myosin is attracted to the site by an attractive force and attaches to the site [Figs. 1(d) to 1(a) or Figs. 1(d) to 1(e)] with a rate constant of k_{on} [Fig. 1(h)]. Just after the attachment, the myosin changes its conformation by releasing the stored energy of $K\Delta^2/2$ in the strain and generates a force again.

Although the myosin cannot pass backward binding sites in model 1, the myosin can pass them in model 2 by virtue of the position-dependent attachment rate constant. Therefore, the sliding motion seems more natural in model 2 [see Fig. 1(j)] than in model 1 [Fig. 1(i)].

C. Introducing fluctuation in step size

We introduce the fluctuation in step size as follows. In both models 1 and 2, the step size Δ is defined as a stochastic variable whose probability density function is given as

$$P(\Delta)=\begin{cases}1/(2w), & \Delta_m-w\le\Delta\le\Delta_m+w,\\ 0 & \text{otherwise},\end{cases} \tag{2}$$

where w (≥ 0) is the fluctuation width and Δ_m is the mean step size. We assume that the step size is positive ($\Delta\ge 0$). Therefore, the fluctuation width must be smaller than the mean step size ($w\le\Delta_m$). We use the uniform density function rather than a Gaussian function because it is easy to confine the step size to the positive domain.

D. Introducing a heterogeneous filament

In the basic motional models, the distance between binding sites for myosins, L, is uniform. However, we also consider the sliding motion along a heterogeneous actin filament, on which binding sites for myosins are distributed not uniformly, but randomly, in space. A motor moving along such a heterogeneous filament, or a disordered track, has been previously studied [24–26]. Here we consider the case in which the probability density function of L is given as

$$\psi(L)=\begin{cases}1/(2\eta), & L_m-\eta\le L\le L_m+\eta,\\ 0 & \text{otherwise},\end{cases} \tag{3}$$

where L_m is the mean distance between binding sites, and η (≥ 0) is the width of fluctuation in L. We define the heterogeneity of this filament as η/L_m.

III. RESULTS

A. Sliding velocity

We can derive the analytical expression for the mean sliding velocity of a myosin-cargo system in model 1 as follows. The mean sliding velocity can be expressed as

$$v = \left(\sum_{i=1}^{N} l_i\right) \Big/ \left(\sum_{i=1}^{N} t_i\right) = \langle l\rangle/\langle t\rangle, \tag{4}$$

where l_i is the displacement produced by the ith force generation cycle [Figs. 1(a) to 1(a) or Figs. 1(a) to 1(e)], t_i is the time required for this displacement, N is the number of cycles, and $\langle\cdot\rangle$ represents an ensemble average over the cycles. Both l_i and t_i are stochastic variables, and the second equality in Eq. (4) is justified when $N \gg 1$.

$\langle l\rangle$ is calculated as follows. Because the myosin-cargo system can attach to either of the two binding sites, the forward and the backward ones [Figs. 1(e) and 1(a), respectively], l_i is 0 or L when $0 \le \Delta \le L$, and L or $2L$ when $L \le \Delta \le 2L$. The case of $\Delta > 2L$ is not considered because we consider the case of $0 \le \Delta_m \le L$ and $0 \le w \le \Delta_m$. The probability that the myosin attaches to the forward binding site is given as $p_f = \Delta/L$ when $0 \le \Delta \le L$, and $p_f = (\Delta - L)/L$ when $L \le \Delta \le 2L$. Therefore,

$$\langle l\rangle = p_f L + (1 - p_f) \times 0 = \frac{\Delta}{L} L = \Delta, \tag{5}$$

for $0 \le \Delta \le L$, and

$$\langle l\rangle = p_f 2L + (1 - p_f)L = \frac{\Delta - L}{L} 2L + \left(1 - \frac{\Delta - L}{L}\right) L = \Delta, \tag{6}$$

for $L \le \Delta \le 2L$. Therefore, we have $\langle l\rangle = \Delta$ for $0 \le \Delta \le 2L$.

On the other hand, $\langle t\rangle$ is calculated as follows: t_i is the sum of $t_i^{(1)}$ and $t_i^{(2)}$, where $t_i^{(1)}$ is the time taken to attach to one binding site by diffusion and $t_i^{(2)}$ is the duration time of an attachment. The former is calculated as a first passage time during which the myosin-cargo system that is positioned within a domain of $[X_B, X_B + L]$ leaves that domain, where X_B is the position of a binding site. Theoretically, its mean value can be derived as the mean first passage time (MFPT) required for a Brownian particle that is initially positioned at $\Delta' \equiv \Delta - jL$ ($j = 0$ or 1) to leave the domain of $[0, L]$ by diffusion, where j is determined by the value of Δ; $j = 0$ when $0 \le \Delta \le L$, and $j = 1$ when $L < \Delta \le 2L$. The MFPT is given as

$$\langle t^{(1)}\rangle = M \equiv \frac{1}{2D} \Delta'(L - \Delta'), \tag{7}$$

when the diffusion constant is D [27]. The latter, i.e., $t^{(2)}$, is also a stochastic variable, and its mean value is given as $1/\nu$. Therefore, we have

$$\langle t\rangle = \langle t^{(1)}\rangle + \langle t^{(2)}\rangle = \frac{1}{2D} \Delta'(L - \Delta') + \frac{1}{\nu}. \tag{8}$$

Substituting the expressions of $\langle l\rangle$ and $\langle t\rangle$ into Eq. (4), we have the mean sliding velocity of the system as

$$v = \frac{\Delta}{\Delta'(L - \Delta')/(2D) + 1/\nu}, \tag{9}$$

where we can replace Δ' by Δ because $0 \le \Delta \le L$ in the case of no step size fluctuation. Figure 2(a) shows both a theoretical curve of v (continuous curve) and numerically calculated velocities (closed circles), when $L = 36$ nm, $\nu = 0.1$ ms^{-1}, and $D = 4$ nm^2 ms^{-1}.

In the case of model 2, we numerically calculate the mean sliding velocities for several values of step size. When the myosin attaches to the actin filament, we use Eq. (1). Otherwise, we use a simple diffusion equation (not shown). The simulations are performed using the following values: $L = 36$ nm, $r = 0.5$ nm, $\gamma = 1$ μg ms^{-1}, $k_{\mathrm{off}} = 1$ ms^{-1}, $k_{\mathrm{on}} = 1$ ms^{-1}, and h (unit step for calculation) $= 1$ μs. Figure 2(b) shows the relation between step size and the velocity in the case of the constant myosin stiffness of $K = 5$ pN nm^{-1} (closed circles). The relation is fundamentally similar to that of model 1, although the velocity when $\Delta \simeq L = 36$ nm is much smaller. We have also calculated the sliding velocity in the case of constant potential energy U (data not shown). In this case, the myosin stiffness K is given as $K = 2U/\Delta^2$, but the relation between step size and the velocity is also fundamentally identical to that of model 1.

B. Effect of fluctuation in step size

In the presence of a fluctuation in step size, the mean sliding velocities are different from those without the fluctuation in both models 1 and 2. Figures 2(a) and 2(b), respectively, show the mean velocity with the fluctuation whose width is equal to the mean step size (i.e., $w = \Delta_m$) in models 1 and 2 (open circles). These velocities are greater than those without fluctuation (closed circles) in both models, when the step size is smaller than about 27 nm. In Figs. 2(c) and 2(d), the relation between the fluctuation width and the mean sliding velocity is shown for six different mean step sizes in models 1 and 2, respectively. When the mean step size Δ_m is 5.4, 10.8, 18, and 25.2 nm, the sliding velocity increases with the fluctuation width w and has the maximal value at $w = \Delta_m$. On the other hand, when Δ_m is 28.8 and 32.4 nm, the sliding velocity has a peak at a moderate value of $w \neq \Delta_m$. For example, when $\Delta_m = 18$ nm in model 1 [see closed squares in Fig. 2(c)], the mean velocity has its maximum (0.48 μm s^{-1}) at $w = 18$ nm. When $\Delta_m = 32.4$ nm in the same model, the velocity has its maximum (1.3 μm s^{-1}) at $w = 3.6$ nm.

To analyze the dependence of the sliding velocity on the fluctuation width in detail, we derive the expression for the mean velocity v as a function of the width w in model 1. When the step size fluctuates uniformly within a domain of $[\Delta_m - w, \Delta_m + w]$, the mean sliding velocity is given as

$$v = \frac{\langle \Delta\rangle}{\langle M\rangle + 1/\nu}. \tag{10}$$

Here we define

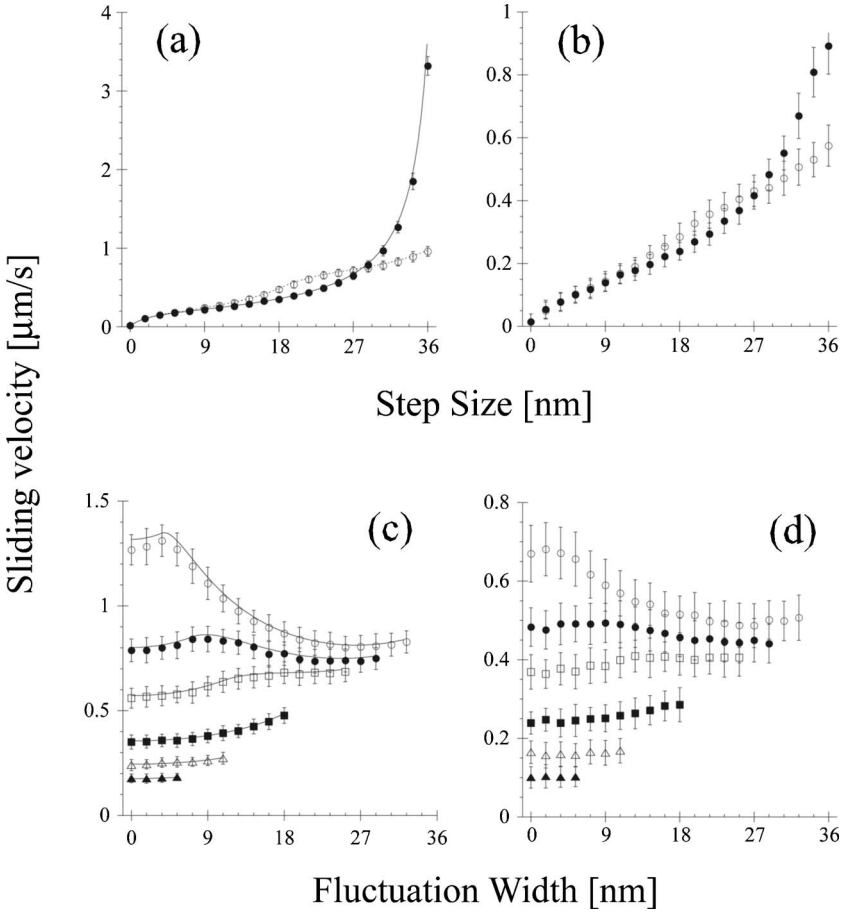

FIG. 2. Sliding velocity. (a), (b) Sliding velocities plotted against the step size with (open circles) and without (closed circles) the fluctuation in step size in models 1 and 2, respectively. The applied fluctuation width is equal to the step size (i.e., $w=\Delta_m$) in both models. (c) and (d) Sliding velocities plotted against the fluctuation width of step size when the mean step size is 5.4 nm (closed triangles), 10.8 (open triangles), 18 (closed squares), 25.2 (open squares), 28.8 (closed circles), and 32.4 nm (open circles) in models 1 and 2, respectively. For the calculations, $L=36$ nm and $D=4$ nm^2 ms^{-1} are used in both models. In addition, $\nu=0.1$ ms^{-1} is used in model 1 [(a) and (c)] and $\gamma=1$ μg ms^{-1}, $k_{\text{off}}=1$ ms^{-1}, $k_{\text{on}}=1$ ms^{-1}, $r=0.5$ nm, and $K=5$ pN nm^{-1} are used in model 2 [(b) and (d)]. Theoretical curves are overlaid on the data of model 1 [(a) and (c)]. Data show mean ± standard deviation for 100 runs in each point.

$$\langle \Delta \rangle \equiv \int \Delta P(\Delta) d\Delta = \frac{1}{2w} \int_{\Delta_m - w}^{\Delta_m + w} \Delta \, d\Delta = \Delta_m \tag{11}$$

and

$$\langle M \rangle \equiv \int M P(\Delta) d\Delta = \int \frac{1}{2D} \Delta'(L - \Delta') P(\Delta) d\Delta, \tag{12}$$

where $P(\Delta)$ and M are given, respectively, by Eqs. (2) and (7). Because the integral in Eq. (12) includes Δ', $\langle M \rangle$ depends on the value of $\Delta_m + w$, when $0 \le \Delta_m + w \le L$, we have

$$\langle M \rangle = \frac{1}{2w} \int_{\Delta_m - w}^{\Delta_m + w} \frac{1}{2D} \Delta(L - \Delta) d\Delta = \frac{1}{2D} \Delta_m (L - \Delta_m) - \frac{w^2}{6D}. \tag{13}$$

When $L < \Delta_m + w \le 2L$, we have

$$\begin{aligned} \langle M \rangle &= \frac{1}{2w} \left[\int_{\Delta_m - w}^{L} \frac{1}{2D} \Delta(L - \Delta) d\Delta + \int_{0}^{\Delta_m + w - L} \frac{1}{2D} \Delta(L - \Delta) d\Delta \right] \\ &= \frac{1}{4wD} \left\{ (\Delta_m - L)^2 (L - 2w) + w^2 \left(L - \frac{2}{3} w \right) \right\}. \end{aligned} \tag{14}$$

Thus, the mean sliding velocity with the step size fluctuation is given as

$$v = \frac{\Delta_m}{\Delta_m (L - \Delta_m)/(2D) - w^2/(6D) + 1/\nu} \tag{15}$$

when $0 \le \Delta_m + w \le L$, and

$$v = \frac{\Delta_m}{[(\Delta_m - L)^2 (L - 2w) + w^2 (L - 2w/3)]/(4Dw) + 1/\nu} \tag{16}$$

when $L < \Delta_m + w \le 2L$. In Fig. 2(c), we overlay these functions on the numerically calculated data points (continuous curves). We also overlay the theoretical curve for the velocity in the case of $w=\Delta_m$ [dotted curve in Fig. 2(a)] on the numerically calculated ones [open circles in Fig. 2(a)]. Equation (15) equals Eq. (9) when $w=0$. Because $\langle M \rangle$ depends on w, whereas $\langle \Delta \rangle$ does not, the increase in the mean sliding velocity is caused by the decrease in the denominator of Eq. (10), the mean time taken for a force generation cycle, and not by the increase in its numerator, the mean displacement made by the cycle, and vice versa.

When the model parameters are normalized with L and ν, we have the dimensionless expression for the mean sliding velocity as

$$u = \frac{\delta}{1 + (\delta - \delta^2 - \omega^2/3)/(2Q)} \equiv u_1(\omega) \tag{17}$$

when $0 \le \omega \le 1 - \delta$, and

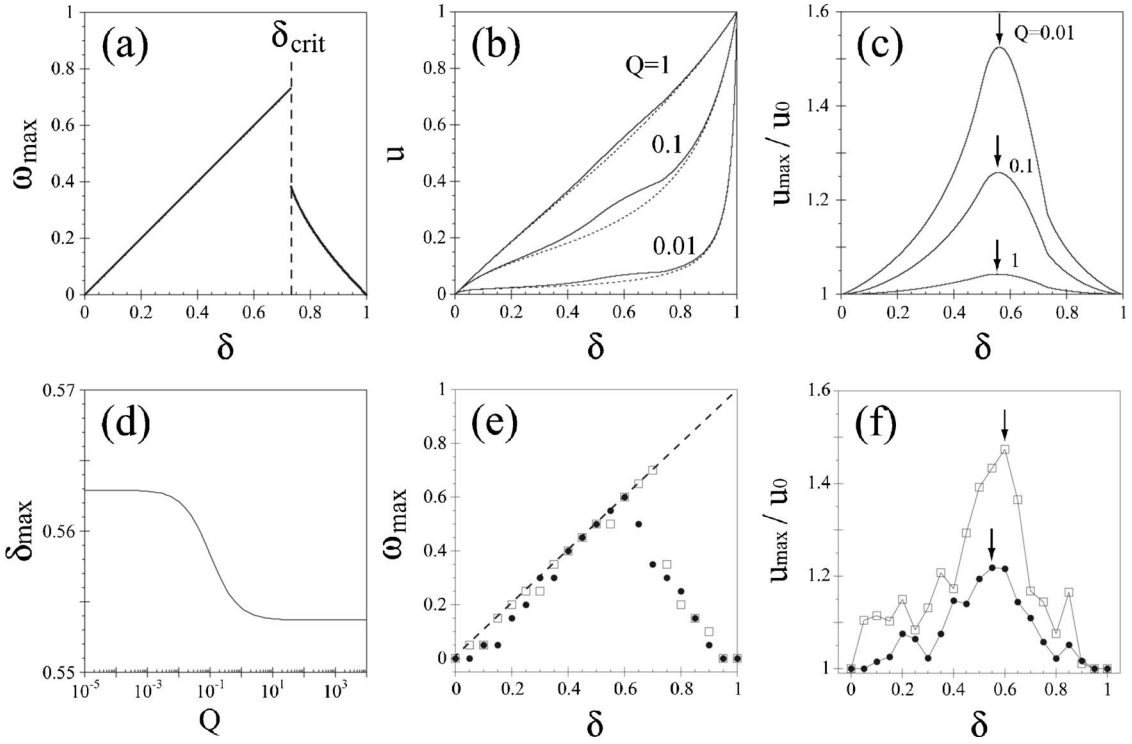

FIG. 3. Maximization of the sliding velocity due to the fluctuation in step size. (a) Dimensionless fluctuation width that maximizes the sliding velocity $\omega_{\max}$ plotted against the dimensionless step size δ. Its dependence on δ changes at $\delta=\delta_{\mathrm{crit}}=0.7317$. The derivation of this critical value is given in the text. (b) Maximized sliding velocity (continuous curves) and the velocity without the fluctuation in step size (dotted curves) plotted against δ. Several dimensionless diffusion constants ($Q=0.01$, 0.1, and 1 from bottom to top) are used for the calculations. (c) Gain in the sliding velocity due to the fluctuation in step size plotted against δ for several diffusion constants ($Q=0.01$, 0.1, and 1 from top to bottom). The gain has a single peak at $\delta=\delta_{\max}$ (arrows). (d) The value of $\delta_{\max}$ plotted against the dimensionless diffusion constant Q. (e) Relation between $\omega_{\max}$ and δ in model 2. $\omega_{\max}$ is determined with the precision of 0.05. For calculations, $K=5$ pN nm^{-1}, $L=36$ nm, $\gamma=1$ μg ms^{-1}, $k_{\mathrm{off}}=1$ ms^{-1}, $k_{\mathrm{on}}=1$ ms^{-1}, $r=0.5$ nm, and $D=0.4$ nm^2 ms^{-1} (open rectangles) or 4 nm^2 ms^{-1} (closed circles) are used. The line $\omega_{\max}=\delta$ is overlaid on the data (dashed line). (f) Gain in the sliding velocity plotted against δ in model 2. The gains are obtained using the ratios of the mean velocity when $\omega=\omega_{\max}$ to that when $\omega=0$, where the values of $\omega_{\max}$ are given in (e). For calculations, $D=0.4$ nm^2 ms^{-1} (open squares) and 4 nm^2 ms^{-1} (closed circles) are used. The other parameter values are the same as those used in (e). The gains have their maximum values at $\delta=0.60$ and 0.55 when $D=0.4$ and 4 nm^2 ms^{-1}, respectively (arrows).

$$u=\frac{\delta}{1+[(1-\delta)^2(1-2\omega)+\omega^2(1-2\omega/3)]/(4Q\omega)}\equiv u_2(\omega) \tag{18}$$

when $1-\delta<\omega\le\delta$, where $u\equiv v/(L\nu)$, $\delta\equiv\Delta_m/L$, $\omega\equiv w/L$, and $Q\equiv D/(L^2\nu)$. $u_1(\omega)$ and $u_2(\omega)$ are defined as functions of ω. The graphs of u plotted against δ when $Q=0.01$, 0.1, and 1 are shown in the dotted curves in Fig. 3(b). Note that $u_2(\omega)$ is applied when $0.5<\delta\le 1$. In the following, we use dimensionless expressions to derive the conditions for maximizing the sliding velocity, and so forth.

C. Maximizing sliding velocity attributable to fluctuation in step size

1. Conditions of maximizing sliding velocity

As mentioned previously, the fluctuation width that maximizes the mean sliding velocity depends on the mean step size. What is the relation between the fluctuation width and the mean step size? To answer this, we use the derived dimensionless expressions for the mean sliding velocity u [Eqs. (17) and (18)] and calculate the dimensionless fluctuation width that maximizes the velocity, $\omega_{\max}$, for each dimensionless mean step size δ. Figure 3(a) shows the result, which is expressed as

$$\omega_{\max}(\delta)=\begin{cases}\delta, & 0\le\delta\le\delta_{\mathrm{crit}},\\ \omega^*, & \delta_{\mathrm{crit}}<\delta\le 1,\end{cases} \tag{19}$$

where ω^* is a function of δ and is given by the solution of $\partial u_2/\partial\omega=0$ that also satisfies $\partial^2 u_2/\partial\omega^2<0$ and $1-\delta<\omega<\delta$. Using the derived ω^*, δ_{crit} is given by the solution of $u_2(\omega^*(\delta))=u_2(\delta)$. The solution is derived numerically as 0.7317. Because ω^* is derived independently of Q, δ_{crit} is independent of Q.

We also identify $\omega_{\max}$ in model 2 with the precision of 0.05, corresponding to the width of 1.8 nm [Fig. 3(e)]. As expected from the theoretical results of model 1 [Fig. 3(a) and Eq. (19)], $\omega_{\max}$ is equal to δ when $\delta\le 0.7$ and $\delta\le 0.6$ in the case of $D=0.4$ nm^2 ms^{-1} [open squares in Fig. 3(e)] and 4 nm^2 ms^{-1} [closed circles in Fig. 3(e)], respectively.

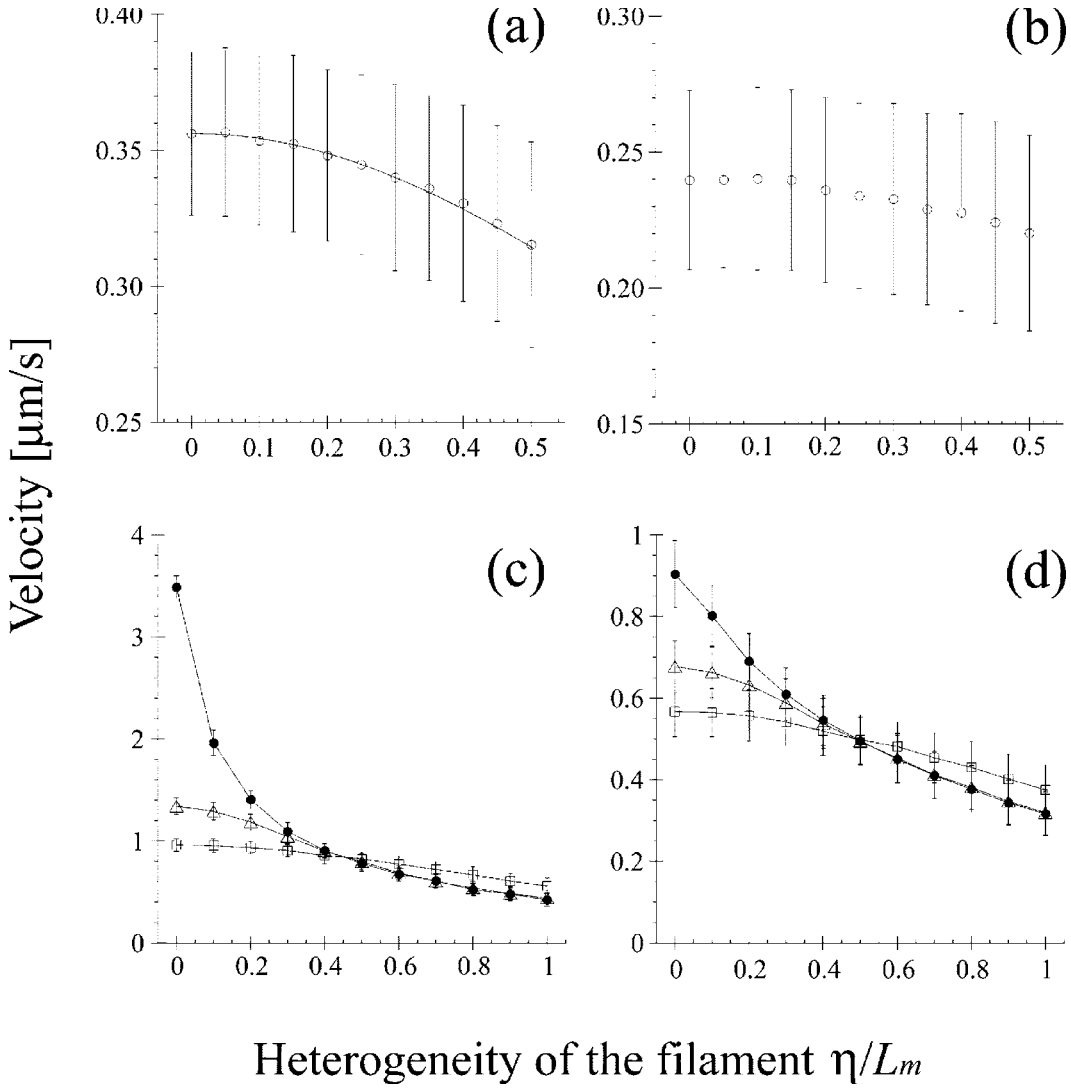

FIG. 4. Sliding velocity along the heterogeneous filament. (a), (b) Velocities plotted against the heterogeneity of the filament η/L_m in the absence of the fluctuation in step size in models 1 and 2, respectively. For calculations, $L_m=36$ nm, $\Delta=18$ nm, and $D=4$ nm^2 ms^{-1} are used in both models. $\nu=0.1$ ms^{-1} is used in model 1 and $\gamma=1$ μg ms^{-1}, $k_{\mathrm{off}}=1$ ms^{-1}, $k_{\mathrm{on}}=1$ ms^{-1}, $r=0.5$ nm, and $K=5$ pN nm^{-1} are used in model 2. Theoretical curve is overlaid on the data of model 1. Data show mean ± standard deviation for 1000 runs in each point. (c), (d) Velocities plotted against the heterogeneity in the presence of the fluctuation in step size under the special condition of $L_m=\Delta_m=36$ nm in models 1 and 2, respectively. The fluctuation width is 0 (closed circles), 9 (open triangles), and 36 nm (open squares). The other parameter values are the same as those used in (a) and (b), respectively. Data show mean ± standard deviation for 100 (c) and 1000 (d) runs in each point.

2. Gain in sliding velocity

The relation between the mean step size δ and the maximized sliding velocity caused by the fluctuation in step size, $u_{\max}$ (the velocity at $\omega=\omega_{\max}$), is shown for several diffusion constants in Fig. 3(b) (continuous curves). For comparison, the velocities without step size fluctuation, u_0, for each diffusion constant are also shown in the same figure (dotted curves).

The gain in the sliding velocity, defined as $u_{\max}/u_0$, varies with δ and Q. Figure 3(c) shows the gains plotted against δ for each diffusion constant. This is expressible as a function of δ;

$$\frac{u_{\max}}{u_0}=\begin{cases}u_1(\delta)/u_1(0), & 0\le\delta\le 0.5,\\ u_2(\delta)/u_1(0), & 0.5\le\delta\le\delta_{\mathrm{crit}},\\ u_2(\omega^*)/u_1(0), & \delta_{\mathrm{crit}}\le\delta\le 1.0.\end{cases} \tag{20}$$

It has a single peak at $\delta=\delta_{\max}$ [arrows in Fig. 3(c)], which is determined as the solution of

$$\frac{\partial}{\partial\delta}\left(\frac{u_2(\delta)}{u_1(0)}\right)=0 \tag{21}$$

that satisfies $0.5\le\delta_{\max}\le\delta_{\mathrm{crit}}$. The calculated value of $\delta_{\max}$ is plotted against the dimensionless diffusion constant Q in Fig. 3(d). The value depends on Q, but within the small domain

of [0.5537, 0.5629]. Therefore, the fluctuation in step size affects the sliding velocity most strongly and the gain in the velocity is largest when $\delta=\delta_{\max}\simeq 0.56$.

Figure 3(f) shows the gain plotted against δ in model 2. The dimensionless step size that maximizes the gain is 0.60 when $D=0.4\ \mathrm{nm}^2\ \mathrm{ms}^{-1}$, and 0.55 when $D=4\ \mathrm{nm}^2\ \mathrm{ms}^{-1}$ [arrows in Fig. 3(f)]. These values correspond to $\delta_{\max}$ in model 1.

D. Effect of heterogeneous filament

When the system slides along the heterogeneous filament, the sliding velocity decreases with increasing heterogeneity η/L_m in both models, where η is the width of fluctuation in L, the distance between binding sites for myosins, and L_m is the mean value of L [see Eq. (3)]. Figures 4(a) and 4(b), respectively, show the dependence of the mean sliding velocity on η/L_m for models 1 and 2.

The decrease in the mean velocity is explainable as follows. For simplicity, we consider model 1 when $0\le\Delta\le L_m-\eta$: the step size is always smaller than the distance between binding sites. Let λ be the distance between adjacent binding sites, termed BS1 and BS2, on a heterogeneous filament whose heterogeneity is η/L_m. By definition, λ is a value between $L_m-\eta$ and $L_m+\eta$, which does not vary in time. The myosin attached to BS1 repeats the force generation cycles [Figs. 1(a)–1(e)] until it reaches the adjacent forward binding site BS2. Consequently, if λ, the distance between BS1 and BS2, is much greater than the step size, the myosin repeats many cycles before it reaches BS2. In contrast, if λ is as small as the step size, the myosin reaches BS2 easily in a single cycle. The mean number of force generation cycles needed for the myosin to reach BS2 is given as

$$n=1\times p_f+2\times p_f(1-p_f)+3\times p_f(1-p_f)^2+\cdots=1/p_f=\lambda/\Delta, \tag{22}$$

where $p_f=\Delta/\lambda$ is the probability that the myosin attaches to the forward binding site.

Let $P_L(\lambda)d\lambda$ be the probability that the distance between a binding site on which a myosin binds and the adjacent binding site in front is found between λ and $\lambda+d\lambda$. When the binding sites are distributed uniformly along the filament, $P_L(\lambda)=\delta(\lambda-L)$ is derived intuitively, where L is the uniform interval of the binding sites and $\delta(\cdot)$ is the Dirac delta function. In the case of a heterogeneous filament whose heterogeneity is η/L_m, $P_L(\lambda)$ is proportional to $\psi(\lambda)$, as defined by Eq. (3) and n derived above. Therefore, P_L has the form of $Cn\psi$, where C is a normalization constant. To meet the condition of $1=\int P_L(\lambda)d\lambda$, $C=\Delta/L_m$ is given. Thus,

$$P_L(\lambda)=\frac{\Delta}{L_m}\frac{\lambda}{\Delta}\psi(\lambda)=\frac{\lambda}{2\eta L_m} \tag{23}$$

when $L_m-\eta\le\lambda\le L_m+\eta$, and $P_L(\lambda)=0$ otherwise. Using this probability distribution function, we can calculate the mean velocity of the system sliding along the heterogeneous filament:

$$v=\frac{\langle\Delta\rangle}{\langle M\rangle+1/\nu}=\frac{\int\Delta P_L(\lambda)d\lambda}{\int MP_L(\lambda)d\lambda+1/\nu}=\frac{\Delta}{\Delta[L_m-\Delta+(L_m/3)(\eta/L_m)^2]/(2D)+1/\nu}, \tag{24}$$

where M is given by Eq. (7). The mean velocity decreases as the heterogeneity η/L_m increases because of the increased mean of the MFPT, $\langle M\rangle$, of the myosin. The increase of $\langle M\rangle$ is caused mainly by the increase in the number of repeated force generation cycles, or the number of futile cycles. This function is overlaid on the numerically calculated data of model 1 [see Fig. 4(a)].

In the special case that the mean step size is equal to the mean distance between binding sites, i.e., $\Delta_m=L_m$, we calculate the dependence of the sliding velocity on the heterogeneity. Figure 4(c) shows the results when the width of the fluctuation in step size is zero (closed circles), small (open triangles), and large (open squares) in model 1. The loss of the sliding velocity attributable to the heterogeneity of the filament is very large in the system without fluctuation in step size. However, the loss becomes very small when the step size fluctuates. We obtain similar results in model 2 [see Fig. 4(d)]. The implications of these results are discussed in Sec. IV.

IV. DISCUSSION

We have analytically derived and numerically calculated the sliding velocities of a system driven by a single myosin molecule whose step size fluctuates for each force generation. Subsequently, we found that the system can slide faster than the system without fluctuation in step size. The appropriate fluctuation width that maximizes the sliding velocity is equal to the mean step size when the ratio of mean step size to the distance between binding sites $\delta=\Delta_m/L$ is less than $\delta_{\mathrm{crit}}\simeq 0.73$. We have also shown that the gain in sliding velocity depends on δ and has a peak at $\delta=\delta_{\max}\simeq 0.56$.

In Table I, the mean step sizes (Δ_m) and widths of fluctuation in step size (w) estimated with three available single-molecule experimental data sets are shown [13,17,18], where we assume that the distance between binding sites L is equal to 36 nm: the half period of the actin filament. All the estimated ratios of mean step sizes to L (the column of Δ_m/L) are less than $\delta_{\mathrm{crit}}\simeq 0.73$. Therefore, the appropriate fluctuation width that maximizes the sliding velocity should be equal to the mean step size. The column of $w_{\max}$ in Table I shows that the estimated fluctuation width w is nearly equal to $w_{\max}$, unexpectedly, in the case of skeletal muscle myosins. This near equivalence implies that these myosins satisfy the conditions of maximizing sliding velocity with fluctuation in step size for a given mean step size.

On the other hand, estimated values of Δ_m/L deviate from $\delta_{\max}\simeq 0.56$, particularly for the second example in Table I [18]. That fact means that the gain in sliding velocity attributable to the fluctuation in step size is not optimized. In other

words, the system is not optimized for using fluctuation in step size to increase the sliding velocity. However, we note that the value of $\delta_{\max} \simeq 0.56$ is applicable to the system driven by a single myosin molecule. The optimized ratio of the mean step size to the distance between binding sites $\delta_{\max}$ is considered to differ from 0.56 for a system that is driven by several or numerous myosins, such as a muscle system. Actually, we calculated the sliding velocity of a system driven by several myosins and found that the optimized ratio shifts to around 0.15 when the number of myosins is more than 50.[2] Therefore the ratio of $\Delta_m/L=0.15$, which is estimated in the second example, implies that the system driven by these myosins might use the fluctuation in step size maximally to increase the sliding velocity.

We also found benefits of the fluctuation in step size on the sliding motion aside from increasing its velocity. The conditions in which the system in both models slides at the maximum velocity are $\Delta=L$ and $w=0$; the step size is equal to the distance between binding sites and not fluctuating. These conditions are true when L is constant, i.e., when the binding sites for myosins are distributed uniformly and fixed. When the binding sites are distributed randomly, however, the sliding velocity along this heterogeneous filament decreases drastically as the heterogeneity increases [closed circles in Fig. 4(c)]. In addition, when the heterogeneity becomes large, such as $\eta/L_m=1$, the mean sliding velocity in the case of $\omega=\delta$ is larger than that in the case of $\omega=0$ in both models [Figs. 4(c) and 4(d)]. More importantly, the loss in the sliding velocity that is attributable to the heterogeneity in the filament is small when $\omega=\delta$, in comparison with the case without fluctuation in step size [open squares in Figs. 4(c) and 4(d)]. In other words, the system can slide along the heterogeneous filament with a velocity that is comparable to that in the homogeneous filament when a fluctuation in step size exists. This robustness against the spatial fluctuation in the filament is inferred as one benefit of the fluctuation in step size.

In the present models, we have assumed that the cargo and the myosin are rigidly connected. However, in real systems such as muscle systems, the linkage between the cargo and the myosin can be flexible. In that case, (i) there is a time delay in the response of the cargo to the conformational change of the myosin, and (ii) the diffusion of the myosin, not the myosin-cargo system, determines the dynamics of the sliding motion. If the response time of the cargo is much larger than the duration of attachment of a myosin to an actin filament, the sliding motion of the myosin-cargo system will be different from the one discussed in this paper.

Comparing example experimental data with the predictions derived from models, it is suggested that biological systems, such as a muscle system, might use the benefits of the fluctuation in step size in actin-myosin sliding motion. These benefits include (i) increasing, or maximizing, mean sliding velocities; and (ii) stabilizing velocity sliding along possible heterogeneous filaments. The present study revealed basic effects of the fluctuation in step size on the sliding motion. These results are applicable to micromachines that must function in environments where the thermal fluctuation cannot be neglected, particularly for the purpose of sliding along the heterogeneous structure. We hope that further theoretical studies on systems driven by several or more numerous myosins will elucidate the effect of the observed fluctuations in step size in actual biological conditions.

[2]These results were obtained when the myosins were connected with a linear elastic spring. The stiffness and rest length of the spring were 25 pN/nm and 43.5 nm, respectively. Generally the optimized ratio depends on the model conditions. The effect of fluctuation in step size on the sliding velocity of the system driven by several myosins will be presented elsewhere.

ACKNOWLEDGMENT

I thank Dr. A. Takamatsu of Waseda University for critically reading a previous draft of the manuscript.

APPENDIX: ESTIMATING THE WIDTH OF FLUCTUATION IN STEP SIZE

Data sets obtained in single-molecule experiments have been used to estimate fluctuation in step size [11]. In one experimental system [1], two beads are attached to the ends of an actin filament. By manipulating these two beads with optical tweezers, the actin filament is positioned on a single myosin molecule that is bound to a third, fixed bead. Because of the interaction, the myosin moves the actin filament along its axis direction. Simultaneously, the trapped beads are also displaced in the same direction. The experimental data obtained using this experimental system constitute a time series of the trapped bead positions. By monitoring the reduction in fluctuation in the bead positions, we can detect the attachment of myosin. Let d be the distance between the mean bead position when the myosin attaches to the actin filament and that when the myosin detaches from the filament. The value of d varies for each myosin attachment; thus it is distributed widely. The mean value of d is believed to correspond to the step size [2], although some researchers have claimed recently that this value might be smaller than the step size [28,29].

Here, we consider the variance of d, σ_d^2. In a previous study [11], we showed that this variance is given as $\sigma_d^2 \simeq A \times \sigma_f^2$, where A is a stiffness correction coefficient, and σ_f^2 is the variance of bead positions in the situation where no myosin attaches to the actin filament. The value of A is given as $(1+K_{\mathrm{trap}}/K_{\mathrm{con}}+2K_{\mathrm{trap}}/K_M)^{-2}$, where K_{trap} is the optical trap stiffness, K_{con} is the connection stiffness between the actin filament and the trapped beads, and K_M is the myosin stiffness.

As an example, we apply the Chara myosin data [17] to the equations. We have $A \simeq (1+K_{\mathrm{trap}}/K_{\mathrm{con}})^{-2}$, if we assume $2K_{\mathrm{trap}} \ll K_M$. Kimura *et al.* used $(1+K_{\mathrm{trap}}/K_{\mathrm{con}})$ for the transformation from d (bead displacement) to Δ (step size) as $\Delta = (1+K_{\mathrm{trap}}/K_{\mathrm{con}}) \times d$ [17]. Therefore, we can estimate the value of $(1+K_{\mathrm{trap}}/K_{\mathrm{con}})$ from the data presented there (note that K_{junction} in their paper corresponds to K_{con} here.). Using the experimental data of $\Delta=18$ nm and $d \pm$ standard deviation $=12.4 \pm 10.4$ nm (under the conditions of [ATP]$=1000$ μM, [ADP]$=0$ μM, and $K_{\mathrm{trap}}=0.05$ pN nm^{-1}),

we have $A=(\Delta/d)^{-2}=(18/12.4)^{-2}=0.47$. On the other hand, σ_f^2 is given as $(k_BT/2)\times[1/K_{\mathrm{trap}}+1/(K_{\mathrm{trap}}+K_{\mathrm{con}})]$ [11], where k_B is the Boltzmann constant and T is the absolute temperature. Substituting $k_B=1.38\times10^{-2}$ g nm^2/s^2 K, $T=300$ K, $K_{\mathrm{trap}}=0.05$ pN nm^{-1}, and $K_{\mathrm{con}}=K_{\mathrm{trap}}/(\Delta/d-1)=0.05/(18/12.4-1)=0.11$ pN nm^{-1}, we have $\sigma_f^2=54.3$ nm^2. Consequently, the presumed variance of the bead displacement is given as $\sigma_d^2=A\times\sigma_f^2=0.47\times54.3=25.5$ nm^2. However, the experimentally estimated variance of the bead displacement is $(10.4)^2=108$ nm^2 (see Table 1 of Ref. [17]; under the conditions of [ATP]=1000 μM, [ADP]=0 μM, and $K_{\mathrm{trap}}=0.05$ pN nm^{-1}).

Therefore, the expected variance (25.5 nm^2) is much smaller than the experimentally obtained variance (108 nm^2). We introduce the fluctuation in step size [11] to explain the discrepancy between these two values. The variance of the bead displacement is given as $\sigma_d^2\simeq A\times(\sigma_f^2+\sigma_\Delta^2)$ if the step size is a stochastic variable whose variance is given as σ_Δ^2. Therefore, by adjusting the value of σ_Δ^2, we can reconcile the experimentally obtained variance with the theoretically expected one.

In the case of Chara myosin data sets [17], the variance of the stochastic step size should be $\sigma_\Delta^2=\sigma_d^2/A-\sigma_f^2=10.4^2/0.47-54.3=175.8$ nm^2 to explain the observed variance of the bead displacement. Therefore, the width of the fluctuation in step size has been estimated as $w\equiv(\sigma_\Delta^2)^{1/2}=(175.8)^{1/2}=13$ nm (see the column for w in Table I).

[1] J. T. Finer, R. M. Simmons, and J. A. Spudich, Nature (London) **368**, 113 (1994).
[2] J. E. Molloy, J. E. Burns, J. Kendrick-Jones, R. T. Tregear, and D. C. White, Nature (London) **378**, 209 (1995).
[3] W. H. Guilford, D. E. Dupuis, G. Kennedy, J. Wu, J. B. Patlak, and D. M. Warshaw, Biophys. J. **72**, 1006 (1997).
[4] A. Ishijima, H. Kojima, T. Funatsu, M. Tokunaga, H. Higuchi, H. Tanaka, and T. Yanagida, Cell **92**, 161 (1998).
[5] K. Kitamura, M. Tokunaga, A. H. Iwane, and T. Yanagida, Nature (London) **397**, 129 (1999).
[6] C. Ruff, M. Furch, B. Brenner, D. J. Manstein, and E. Meyhofer, Nat. Struct. Biol. **8**, 226 (2001).
[7] W. Steffen, D. Smith, R. Simmons, and J. Sleep, Proc. Natl. Acad. Sci. U.S.A. **98**, 14949 (2001).
[8] M. Capitanio, M. Canepari, P. Cacciafesta, V. Lombardi, R. Cicchi, M. Maffei, F. S. Pavone, and R. Bottinelli, Proc. Natl. Acad. Sci. U.S.A. **103**, 87 (2006).
[9] A. D. Mehta and J. A. Spudich, Adv. Struct. Biol. **5**, 229 (1998).
[10] T. Yanagida, K. Kitamura, H. Tanaka, A. H. Iwane, and S. Esaki, Curr. Opin. Cell Biol. **12**, 20 (2000).
[11] Y. Kagawa and Y. Tsuchiya, Bull. Math. Biol. **64**, 407 (2002).
[12] R. D. Vale and R. A. Milligan, Science **288**, 88 (2000).
[13] H. Tanaka, A. Ishijima, M. Honda, K. Saito, and T. Yanagida, Biophys. J. **75**, 1886 (1998).
[14] M. Reconditi *et al.*, Nature (London) **428**, 578 (2004).
[15] V. Decostre, P. Bianco, V. Lombardi, and G. Piazzesi, Proc. Natl. Acad. Sci. U.S.A. **102**, 13927 (2005).
[16] M. Morimatsu, A. Nakamura, H. Sumiyoshi, N. Sakaba, H. Taniguchi, K. Kohama, and S. Higashi-Fujime, Biochem. Biophys. Res. Commun. **270**, 147 (2000).
[17] Y. Kimura, N. Toyoshima, N. Hirakawa, K. Okamoto, and A. Ishijima, J. Mol. Biol. **328**, 939 (2003).
[18] C. Veigel, M. L. Bartoo, D. C. White, J. C. Sparrow, and J. E. Molloy, Biophys. J. **75**, 1424 (1998).
[19] J. K. Douglass, L. Wilkens, E. Pantazelou, and F. Moss, Nature (London) **365**, 337 (1993).
[20] J. E. Levin and J. Miller, Nature (London) **380**, 165 (1996).
[21] W. J. Blake, M. Kærn, C. R. Cantor, and J. J. Collins, Nature (London) **422**, 633 (2003).
[22] K. Tawada and K. Sekimoto, Biophys. J. **59**, 343 (1991).
[23] Y. Kagawa, Y. Mizukami, and Y. Tsuchiya, J. Phys. Soc. Jpn. **68**, 1040 (1999).
[24] T. Harms and R. Lipowsky, Phys. Rev. Lett. **79**, 2895 (1997).
[25] Y. Kafri, D. K. Lubensky, and D. R. Nelson, Phys. Rev. E **71**, 041906 (2005).
[26] J. W. Shaevitz, S. M. Block, and M. J. Schnitzer, Biophys. J. **89**, 2277 (2005).
[27] R. L. Stratonovich, *Topics in the Theory of Random Noise* (Gordon and Breach, New York, 1963).
[28] J. Sleep, A. Lewalle, and D. Smith, Proc. Natl. Acad. Sci. U.S.A. **103**, 1278 (2006).
[29] B. Brenner, J. Muscle Res. Cell Motil. **27**, 173 (2006).